Cytotoxicity and global transcriptional responses induced by zinc oxide nanoparticles NM 110 in PMA-differentiated THP-1 cells

Ramia Safar, Zahra Doumandji, Timeh Saidou, Luc Ferrari, Sara Nahle, Bertrand Rihn, Olivier Joubert

Cytotoxicity and global transcriptional responses induced by zinc oxide nanoparticles NM 110 in PMA-differentiated THP-1 cells

Ramia Safar[a#], Zahra Doumandji[a#], Timeh Saidou[a], Alain LeFaou[b], Luc Ferrari[a], Sara Nahlé[a], Bertrand H Rihn[a], Olivier Joubert[a*]

[a] UMR CNRS 7198, Institut Jean Lamour, Faculté de Pharmacie, Université de Lorraine, Nancy, France.

[b] EA 3452 CITHEFOR, Faculté de Médecine, Université de Lorraine, Nancy, France.

[#] both co-authors contributed equally to the work

[*] To whom correspondence should be addressed:

Olivier Joubert,

UMR CNRS 7198 Institut Jean Lamour, 2 Allée André Guinier, 54001 Nancy, France

Phone: (+33) 372 742 694

E-mail: olivier.joubert@univ-lorraine.fr

Abstract

Despite a wide production and use of zinc oxide nanoparticles (ZnONP), their toxicological study is only of limited number and their impact at a molecular level is seldom addressed. Thus, we have used, as a model, zinc oxide nanoparticle NM110 (ZnO110NP) exposure to PMA-differentiated THP-1 macrophages. The cell viability was studied at the cellular level using WST-1, LDH and Alamar Blue® assays, as well as at the molecular level by transcriptomic analysis. Exposure of cells to ZnO110NP for 24 h decreased their viability in a dose-dependent manner with mean inhibitory concentrations (IC_{50}) of 8.1 µg/mL. Transcriptomic study of cells exposed to two concentrations of ZnO110NP: IC_{50} and a quarter of it ($IC_{50}/4$) for 4 h showed that the expressions of genes involved in metal metabolism are perturbed. In addition, expression of genes acting in transcription regulation and DNA binding, as well as clusters of genes related to protein synthesis and structure were altered. It has to be noted that the expressions of metallothioneins genes (*MT1, MT2*) and genes of heat-shock proteins genes *(HSP)* were strongly upregulated for both conditions. These genes might be used as an early marker of exposition to ZnONP. On the contrary, at IC_{50} exposure, modifications of gene expression involved in inflammation, apoptosis and mitochondrial suffering were noted indicating a less specific cellular response. Overall, this study brings a resource of transcriptional data for ZnONP toxicity for further mechanistic studies.

Keywords: zinc oxide nanoparticle, NM110, PMA-differentiated THP-1 cells, transcriptome, cytotoxicity, metallothionein.

1. Introduction

Nanoparticles (NP) of metal oxides are attracting more and more interest and are produced in large quantities. They are widely used in both industrial process and biomedical research (Girigoswami, 2018). Nevertheless, data on their potential toxicity on living organisms remain insufficient, particularly at the molecular level. Zinc oxide nanoparticles (ZnONP) have multiple industrial uses and commercial applications, and it is one of the main NP present in the market due to its many properties. According to the Project on Emerging Nanotechnologies Inventory of nanotechnology-based Consumer Products, ZnONP are present in at least 24 commercialized products, primarily sunscreen formulations, due to its UV- absorbing properties (Vance et al., 2015), with more than 33,000 tons of sunscreens produced containing up to 25 % of ZnONP (Joo and Zhao, 2017). There are many other pharmaceutical and parapharmaceutical applications of ZnONP such as ointments, skin creams, toothpaste, deodorants and formulation of cosmetics. ZnONP have also found industrial applications in rubber, ceramics, optical glasses, paints and plastics (Mishra et al., 2017).

As a result of this numerous applications, toxicity studies on ZnONP have already been investigated by different research groups. Majority of these studies are limited to qualitative data, demonstrating that ZnONP induce an increase in the cell death rate (Farcal et al., 2015), generally associated with inflammation (Sahu et al., 2014), DNA damage, and induction of oxidative stress (Senapati et al, 2015). However, the molecular mechanisms involved in these effects remains undefined. In addition, it has been shown that the importance of the toxic effects of ZnONP is inversely related to size, positive charge and solubility of nanoparticles (Prach et al., 2013; Buerki-Thurnherr et al., 2013). On the other hand, they vary with the cell line used and

macrophages are said to be more sensible when contact with ZnONP than epithelial cells (Farcal et al., 2015), as well as cancer cells when compared to normal cells (Premanathan et al., 2010).

The present study was performed with the objective to study the toxicity of NP on the respiratory system using *in vitro* models. Given that a human pulmonary macrophage cell line does not exist, the model used for this work was the monocytes THP-1 cell line which are differentiated into macrophages by treatment with PMA showing enhanced adherence and phagocytosis. In addition, the major role of macrophage in the innate defense of the body, especially their strong phagocytic capacity, and their presence in many tissues and organs make it a model of choice for many *in vitro* studies for toxicological impacts of NP (Jones CF, Grainger DW, 2009).

Then, this manuscript focuses on the toxicity of uncoated zinc oxide nanoparticles NM110 (ZnO110NP) in PMA-differentiated THP-1 macrophages. ZnO110NP is one of representative manufactured nanomaterials in the priority list (NM-Series) which has been established to be well characterized and tested by the European Commission's Joint Research Centre (JRC) in order to enable innovation and development of safe materials and products. Cell viability was assessed using classical tests of toxicology while the molecular response of these cells was established by transcriptomic analysis.

2. Materials and Methods

2.1. Chemicals

DMEM medium (Dulbecco's Modified Eagle's Medium- high glucose, D1145), fetal bovine serum (F7524), L-glutamine [CAS No. 56-85-9], Penicillin [113-98-4], streptomycin [128-46-1], amphotericin B [1397- 89-3], phorbol 12-myristate 13-acetate (PMA) [1656-9-8], Dulbecco's Phosphate Buffered Saline (PBS) [16561-29-8], trypan blue solution [72-57-1], Ethylenediaminetetraacetic acid disodium salt (EDTA) [6381-92-6], Bovine Serum Albumin (BSA) [9048-46-8], Diethyl pyrocarbonate (DEPC) [150-38-9] were purchased from Sigma-Aldrich® (Saint Quentin Fallavier, France). APC anti-human CD11c and IgG1-APC isotype control were purchased from (BD biosciences, Le Pont de Claix, France). 4-[3-(4-Iodophenyl)-2-(4-nitrophenyl)-2H-5-tetrazolio]-1,3-benzene disulfonate (WST-1) cell proliferation reagent [150849-52-8] and cytotoxicity detection Kit PLUS LDH, were from Roche® (Meylan, France). AlamarBlue® Cell Viability Reagent (DAL1025) was from Invitrogen (Villebon sur Yvette, France). RNA-Solv Reagent® (R6830) from Omega Bio-tek® (Norcross, Geogia). Éthanol 100% [75-17-5], chloroforme [67-66-3], isopropanol [67-68-0] from Carlo Erba Reagents® (Val de Rueil, France).

2.2. Preparation and characterization of nanoparticle suspension

ZnO110NP were obtained from the Joint Research Center (NM 110, JRS). They are suspended in ultrapure water (18 MΩ) at a concentration of 2.56 mg/mL **(Phuyal et al, 2017),** sonicated using a 3-mm probe (Vibracell 75022, Bioblock, Illkirch, France) at 30 % magnitude for 6 min under continuous cooling with ice. Immediately after sonication, ZnO110NP

suspension was physico-chemically characterized and working dilutions in the culture medium were prepared.

The hydrodynamic diameter and size distribution of ZnO110NP suspension, expressed as polydispersity index (PdI), were measured using dynamic light scattering (DLS, Zetasizer™ 3000E, Malvern Instruments Worcestershire, UK). Zeta potential was calculated using the *Smoluchowski's* equation (Sze et al., 2003). All measurements were performed in triplicate at 25 °C.

2.3. Cell culture

THP-1 human monocytic cell line was obtained from American Type Culture Collection (ATCC, TIB-202™, Manassas, VA, USA). Cells were cultured in DMEM medium supplemented with 15 % of heat-inactivated fetal bovine serum, 100 U/mL of penicillin, 100 µg/mL of streptomycin, 0.25 µg/mL of amphotericin and 2 mM of L-Glutamine in incubator at 37°C under 5 % CO_2 atmosphere. They were split every 2-3 days to prevent the cell density from exceeding one million per mL. For each experiment, cells were differentiated into macrophages by exposure to 10 ng/mL (16 nM) of PMA in a plate appropriate to the test for 24 h. The density of 5 x 10^4 cells per mL was respected for all tests.

2.4. Cell phenotype study

After differentiation, cell phenotype was verified by flow cytometry. THP-1 cells were treated with and without PMA in 6 wells UpCell plate (Thermo-Fisher, Illkirch, France). After 24 h, cells were harvested using Versene solution (PBS and EDTA 0.1%). After 5 min of centrifugation at 400 x *g*, cell pellet was resuspended in PBS-BSA. 4 x 10^5 cells were incubated

with fluorescein isothiocyanate (FITC)-labeled monoclonal antibodies against CD11c for 30 min, then washed with PBS-BSA, and were analyzed by flow cytometry (BD Biosciences, Le Pont de Claix, France). Non-differentiated unstained cells were used as control.

2.5. Cytotoxicity study

After treatment with PMA for 24 h, the medium was removed by aspiration and cells were incubated with 0 (control), two times dilution from 20 to 0.6 µg/mL of ZnO110NP in serum free medium for 24 h. The cell viability was checked using WST-1, LDH and, AlamarBlue® assays. Unexposed cells were used as control and considered as having 100 % of cell viability. Six wells and four test replicates were used per culture condition. The inhibitory concentration (IC_{50}) was calculated with the Reed and Muench method (Reed and Muench, 1938).

2.5.1. WST-1 assay

WST-1 (water soluble tetrazolium) assay was performed as previously described (Ronzani et al., 2014). Briefly, after 24 h of exposure to ZnO110NP, cells were incubated with 5 % WST-1 reagent for 2 h at 37 °C. Then, the absorbance was read at 450 nm with 690 nm as reference (iMarkTM Microplate Absorbance Reader, Bio-Rad).

2.5.2. LDH assay

Lactate dehydrogenase (LDH) assay was performed according to manufacturer's instructions. Briefly, after 24 h of exposure to ZnO110NP, cells were incubated with 100 µL of (LDH reaction buffer + substrate) for 30 min at room temperature, Then, 50 µL of stop solution was added and the absorbance was read at 490 nm (iMarkTM Microplate Absorbance Reader, Bio-Rad). For the positive control, cells were exposed to lysis buffer for 15 min before the test.

2.5.3. AlamarBlue® assay

AlamarBlue® assay was performed according to manufacturer's instructions. Briefly, cells were incubated with 10 % of reagent for 3 h at 37 °C. Fluorescence was read at 590 nm after excitation at 560 nm using spectrofluorimetry (JASCO, FMP-825, Bouguenais, France)

2.6. Transcriptomic study

2.6.1. RNA extraction

$1x10^6$ THP-1 cells were exposed, after differentiation, to ZnO110NP at concentrations of the IC_{50} or one fourth of IC_{50} ($IC_{50}/4$) for 4 h using unexposed cells as control. As previously described (Eidi et al., 2012; Safar et al., 2015), total RNA was, then, extracted using RNA-Solv Reagent® according to manufacturer's protocols. The quality of the extracted RNA was assessed by spectrophotometry (BioSpec-nano, Shimadzu) and capillary electrophoresis using RNA 6000 Nano® (2100 Bioanalyzer™, Agilent Technologies, Santa Clara, CA). All RNA samples showed a ratio $A_{260nm}/A_{280nm} > 1.8$ with RNA integrity number (RIN) > 8.

2.6.2. Microarray hybridation

cDNA and Cy3-dye-labeled cRNA synthesis were carried out with 100 ng of total RNA according to the manufacturer protocol (One-Color Microarray-Based Gene Expression Analysis, version 6.6). Then, 600 ng of labelled cRNA were hybridized using Microarray slides (SurePrint G3 Human GE v3 8x60K, Agilent Technologies) at 65 °C during 17 h. After washing, the arrays were scanned by Agilent DNA microarray scanner (Agilent). Acquisition of images and quantification of fluorescence signal as well as primary data analysis were performed using the Agilent Feature Extraction Software version 11.0.1.1.

2.6.3. Bioinformatics analyses

Data were first normalized with Lowess' method using GeneSpring (version 13.0, Agilent Technologies Pty Ltd). Then, a principal component analysis (PCA), was performed using GeneSpring as a quality control step where the outlier's samples were removed. Student's *t*-test followed by Benjamini-Hochberg correction and filtering criteria were then applied to identify genes whose expression level was significantly modified. Genes showing expression changes of at least 1.5-fold change (FC) in either direction as compared to control with $p \leq 0.05$ were considered significantly differentially expressed and were used in the following analysis.

The selected genes were analyzed using the Database for Annotation, Visualization, and Integrated Discovery version 6.8 (DAVID; http://david.abcc.ncifcrf.gov). Indeed, genes were grouped among clusters according to different criteria such as Gene Ontology (GO) terms (GO BP: biological process, GO CC: cellular component, GO MF: molecular function) and pathways (KEGG and BIOCARTA). For the biological interpretation, we have considered GO biological process (GO BP) and pathways with *p*-value ≤ 0.05 within the cluster with Enrichment Score above to 1.3 (Huang da et al., 2009). All raw data of the microarrays are available on NCBI Gene Expression Omnibus database (GEO, http://www.ncbi.nlm.nih.gov/geo/), using the GSE599435 accession number.

2.7. Statistical analysis

Cell viability data are presented as means ± standard error of the mean (SE) of four biological replicates. Statistical differences were determined by one-way analysis of variance (ANOVA) followed by Dunnett's test using Prism software™.

3. Results

3.1. Nanoparticle characterization

The mean hydrodynamic diameter of ZnO110NP was 261.5 ± 4 nm with a polydispersity index of 0.170 ± 0.017 and the zeta potential was +21.6 ± 1.8 mV (Figure 1). **TEM images showed that each unit on NP have at least one dimension less than 100 nm (see Figure S2 in supplementary data). Size of particles was checked by DLS immediately and after 24 hours in the medium of exposure, showing no aggregation nor changes in the size of particles (see Table S7 in supplementary data).**

Figure 1

3.2. Cell phenotype study

The exposure to PMA increase the $CD11c^+$ cells number from 62.9 % to 93.9 % (Figure 2) suggesting that, in our macrophage culture conditions, notable part of the cells was already at least partially differentiated. PMA pretreatment allows uniformity of the cell phenotype before the NP exposure.

Figure 2

3.3. Cytotoxicity study

Whatever the assays (Figure 3), exposure of cells to ZnO110NP for 24 h decreased their viability in a dose-dependent manner. WST-1 (Figure 3A) and AlamarBlue® (Figure 3B) assays

gave similar results and a viability of 9.6 % and 7.5 %, respectively at the higher concentration of ZnO110NP (20 µg/mL). In contrast, for LDH assay (Figure 3C), the decrease of viability with NP concentration was slow and a viability of 42 % was solely reached at 20 µg/mL. However, there was no significant difference in IC_{50} (Figure 3) for the three tests and the mean of 8.1 µg/mL (which correspond to 2.1 µg/cm^2), was considered and retain for the transcriptomic assay.

Figure 3

3.4. Transcriptomic study

Cells were exposed for 4 h to ZnO110NP at concentrations of 2.0 and 8.1 µg/mL: namely, IC_{50}/4 and IC_{50} corresponding to 0.5 and 2.1 µg/cm^2, respectively. PCA analysis showed a clear segregation of results for the three groups corresponding to the three conditions (control, cells exposed to IC_{50}/4, or to IC_{50}) (Figure S1 in supplementary informations). As compared to control, 360 significantly differentially expressed genes were identified following exposure to 2.0 µg/mL of ZnO110NP, a non-cytotoxic concentration. Among them, 33 were up-regulated and 327 were down-regulated. Not surprisingly, the exposure to 8.1 µg/mL of ZnO110NP induced the modification of a far greater number of genes, 3202 genes were differentially expressed with 872 and 2330 up and down-regulated respectively (Table 1). All these genes are listed in the supplementary information Table S1, S2 for 2.0 µg/mL concentration and S3, S4 for 8.1 µg/mL concentration.

Functional Gene Ontology (GO) analysis revealed similar clusters of genes in both exposed cell populations. In fact, cluster containing genes involved in or related to ZnO metabolism was found for both conditions with three identical GO BP, namely “cellular response

to zinc ion", "cellular response to cadmium ion" and "negative regulation of growth" and one KEGG pathway "Mineral absorption". Other clusters of genes with modified responses were also common to both conditions: clusters related to virus, perturbation of gene transcription regulation and to protein synthesis and structure (Figure 4). The lower dose (2.0 µg/mL) of ZnO110NP induced modification gene expression belonging to the clusters related to transduction mechanism, i.e "lipid phosphorylation" cluster. On the contrary, at 8.1 µg/mL, modifications of expression of genes involved in inflammation, apoptosis and mitochondrial suffering were noted indicating a less specific cellular response. The analyzed transcriptomic results are summarized and illustrated in Fig. 4. Biological process (GOTERM_BP) and pathways (KEGG, BIOCARTA) of each cluster were presented in supplementary information table S5 for 2.0 µg/mL concentration and table S6 for 8.1 µg/mL concentration.

Moreover, there were 27 genes whose expression was increased after exposition of cells to both concentrations (Figure 5A). The FC values for majority of these genes vary in dose-dependent manner (Table 2). The STRING 10.5 (Search Tool for the Retrieval of Interacting Genes; http://string-db.org/) database (Szklarczyk et al., 2014) analysis shows that they belong to two families of genes: metallothioneins and heat shock proteins (HSP) (Figure 5B).

Figure 4

Figure 5

Table 2

4. Discussion

The present study was performed with the objective of studying the toxicity of ZnO110NP on the respiratory system using an *in vitro* macrophage model, the PMA-differentiated THP-1 monocytic cell line monocytes. The use of PMA allowed us to uniformize the cell phenotype before NP exposure.

When exposed to ZnO110NP, the viability of THP-1 cells decreased in a dose-dependent manner. Calculated IC_{50} was assessed to 8.1 µg/mL using the three tests. In the same way, Farcal and collaborators (2015) studied ZnO110NP toxicity on nine different cellular types which includes primary human macrophages (HMDM), murine peritoneal macrophage-like cells (RAW264.7) and murine alveolar macrophage-like cells (MH-S). ZnO110NP was highly toxic to all the cellular lines tested. However, the IC_{50} value was > 100 µg/mL for HMDM, 18.40 µg/mL for RAW264.7 and 19.68 µg/mL for MH-S cells using different tests. In our study, PMA-differentiated THP-1 macrophages were more sensitive to ZnO110NP as IC_{50} was found to be 8.1 µg/mL. This difference between IC_{50} values is probably due to the fact that Farcal et al resuspended the NP in water with ethanol and BSA *versus* water alone in our study. Although ZnO110NP have the same size and charge in both studies, a plasma protein corona formation around nanoparticles could probably impair their bioreactivity and make them less toxic (Hussien et al, 2013; Rihn and Joubert, 2015; Hongying et al., 2018) by limiting their uptake by cells. In addition, in ours study, cell exposition to ZnO110NP was performed in serum free medium which would allow the nanoparticles to freely exert their cytotoxicity. Finally, THP-1 is a cancerous cell line, and according to a previous study, ZnONP exhibited much higher cytotoxic effects on malignant cells than on normal cells (Premanathan et al, 2011). Furthermore, Liang et al (2018) studied the cytotoxicity of ZnO110NP on THP-1 macrophages, their observations are

generally in agreement with our results. Other forms of ZnONP exists and are also considered as toxic, this toxicity may differ depending on their physicochemical properties as well as the cellular model being used (Yin et al., 2015; Hanley et al, 2009a; 2008b).

Several studies have proposed different mechanisms to explain the toxicity of ZnONP based on oxidative stress and inflammatory response induction (Roy et al., 2013; De Berardis et al., 2010; Moos et al., 2011). Thus, we decided to study the global transcriptional responses following 4 h exposure to low ($IC_{50}/4$ = 2.0 µg/mL or 0.5 µg/cm^2) or high (IC_{50} = 8.1 µg/mL or 2.1 µg/cm^2) concentrations in order to identify early adverse effects of ZnO110NP. **The zinc concentration was measured in the cells after $IC_{50}/4$ exposure by ICP-AES (see Table S8)**. Indeed, a non-cytotoxic low concentration of ZnO110NP allows us to study the adaptive response, while the cytotoxic high concentration gives a hint of the causes of toxicity and cellular death as shown in Fig. 4. After exposure to the high concentration, the number of genes whose expression significantly changed were much higher than the one observed for the lower one (nearly 10 times). However, in both conditions, we observed clusters of genes associated with "cellular response to zinc and cadmium ions" and "mineral absorption pathway" as also described by Moos et al (2011) using four human cell lines: CaCo-2, RKO, HaCaT, SK Mel-28 following a 4 h-exposure period with 1 and 5 µg/cm^2 of ZnONP. This response was observed regardless of cellular model indicating that these gene clusters could be considered as a specific response to ZnO. Among these genes, we noticed that a Zn efflux transporter gene (*SLC30A1*) and metallothioneins genes (*MT1, MT2*) were strongly activated. So, this response of cells is early and is a sensitive exposure biomarker of ZnONP that has been also observed by Tuomela et al (2013) with three immune cell lines: human monocyte-derived macrophages (HMDM), monocyte-derived dendritic cells (MDDC), and Jurkat T cell leukemia-derived cell line. In

addition, Moos et al demonstrated that this family of genes was also up-regulated following their exposure to soluble Zn^{+2} ($ZnCl_2$). This suggested that this response is related to a liberation of Zn^{+2} by degradation of ZnONP. This might occur in the intravacuolar compartment, an acidic environment created by the lysosomes (Gwak et al., 2015). These results, corresponding to intracellular mechanism of defense against to Zn^{2+} are in favor of the hypothesis that states that ZnONP dissolution occurs inside the endosomes (Senapati et al., 2015) and less likely in the extracellular compartment (Buerki-Thurnherr et al., 2013). This intracellular hypothesis, is reinforced by the non-specific response, namely, over expression of heat shock proteins (*HSPA6, HSPA1A,* and *HSPA1B*) genes at 6912, 1586, 461 times respectively, which was observed after exposure to both Zn110ONP concentrations representing a well-known stress response to metal toxicity (Bauman et al., 1993).

Beside the induction of metal responsive genes, the most characteristic clusters influenced by high and low concentrations of ZnO110NP were related to regulation of gene transcription and DNA binding. This may be not surprising as Zn^{2+} ion is a cofactor in the structure of many zinc finger motif proteins that are transcription factors and of DNA binding proteins. This effect was limited for the lower concentration, but more visible for higher one such as clusters of “DNA damage recognition” and “RNA splicing”. However, for this latter, it is possible that these proteins are subject to disruption by a high concentration of Zn^{2+} (Hartwig, 2001).

In addition, it is only at high concentration that, inflammation and mitochondrial dysfunctions, as well as apoptosis pathway, could be identified indicating a non-specific mechanism of toxicity as shown in several studies using different cellular models (Gao et al., 2016; Wang et al., 2018; Wilhelmi et al., 2013; Chevallet et al., 2016).

1

5. Conclusion

In summary, this study brings additional sources of transcriptional data for ZnONP toxicity for further mechanistic studies. Indeed, exposure of PMA-differentiated THP-1 cells to a low non-cytotoxic ZnONP concentration ($IC_{50}/4$) has shown that they have a cellular metabolic alteration giving specific sensitive markers of exposition related to Zn metabolism. At the high cytotoxic concentration (IC_{50}), markers of cytotoxicity and cell death are not specific but the markers of exposition to Zn are still present. The metallothioneins genes family (*MT1, MT2)* was strongly upregulated in both conditions. **The proteins encoded by these genes are known to** participate in the metabolism of Zn and Cu and in the detoxification of heavy metals (e.g. Cd). Thus, the genes coding these proteins might be used as an early marker of exposition to metallic NP.

Acknowledgement

This work was conducted within Smartnanotox frame, a European Union's Horizon 2020 research and innovation program, grant agreement No. 686098. Authors would like to thank Dr Céline Bonnet for giving access to its microarray scanner.

Conflict of interest

The authors declare that they have no conflicting interests.

References

Bauman, J.W., Liu, J., Klaassen, C.D., 1993. Production of metallothionein and heat-shock proteins in response to metals. Fundam Appl Toxicol. 21(1), 15-22.

Buerki-Thurnherr, T., Xiao, L., Diener, L., Arslan, O., Hirsch, C., Maeder-Althaus, X., Grieder, K., Wampfler, B., Mathur, S., Wick, P., Krug, H.F., 2013. In vitro mechanistic study towards a better understanding of ZnO nanoparticle toxicity. Nanotoxicology. 7(4):402-16. DOI: 10.3109/17435390.2012.666575.

Chevallet, M., Gallet, B., Fuchs, A., Jouneau, P.H., Um, K., Mintz, E., Michaud-Soret, I., 2016. Metal homeostasis disruption and mitochondrial dysfunction in hepatocytes exposed to sub-toxic doses of zinc oxide nanoparticles. Nanoscale. 8(43),18495-18506. DOI: 10.1039/c6nr05306h

De Berardis, B., Civitelli, G., Condello, M., Lista, P., Pozzi, R., Arancia, G., Meschini, S., 2010. Exposure to ZnO nanoparticles induces oxidative stress and cytotoxicity in human colon carcinoma cells. Toxicol Appl Pharmacol. 246(3), 116-127. DOI: 10.1016/j.taap.2010.04.012.

Eidi, H., Joubert, O., Némos, C., Grandemange, S., Mograbi, B., Foliguet, B., Tournebize, J., Maincent, P., Le Faou, A., Aboukhamis, I., Rihn B.H., 2012. Drug delivery by polymeric nanoparticles induces autophagy in macrophages. Int J Pharm. 422 (1-2),495-503. DOI: 10.1016/j.ijpharm.2011.11.020

Farcal, L., Torres Andón, F., Di Cristo, L., Rotoli, B.M., Bussolati, O., Bergamaschi, E., Mech, A., Hartmann, N.B., Rasmussen, K., Riego-Sintes, J., Ponti, J., Kinsner-Ovaskainen, A., Rossi, F., Oomen, A., Bos, P., Chen, R., Bai, R., Chen, C., Rocks, L., Fulton, N., Ross, B., Hutchison, G., Tran, L., Mues, S., Ossig, R., Schnekenburger, J., Campagnolo, L., Vecchione, L., Pietroiusti, A., Fadeel, B., 2015. Comprehensive In Vitro Toxicity Testing of a Panel of Representative Oxide Nanomaterials: First Steps towards an Intelligent Testing Strategy. PLoS One. 10(5):e0127174. DOI: 10.1371/journal.pone.0127174. eCollection 2015.

Gao, F., Ma, N., Zhou, H., Wang, Q., Zhang, H., Wang, P., Hou, H., Wen, H., Li, L., 2016. Zinc oxide nanoparticles-induced epigenetic change and G2/M arrest are associated with apoptosis in human epidermal keratinocytes. Int J Nanomedicine. 11, 3859-3874. DOI: 10.2147/IJN.S107021

Girigoswami, K., 2018. Toxicity of Metal Oxide Nanoparticles. Adv Exp Med Biol. 122, 1048-1099. DOI: 10.1007/978-3-319-72041-8_7.

Gwak, G.H., Lee, W.J., Paek, S.M., Oh, J.M., 2015. Physico-chemical changes of ZnO nanoparticles with different size and surface chemistry under physiological pH conditions. Colloids Surf B Biointerfaces. 127, 137-142. DOI: 10.1016/j.colsurfb.2015.01.021

Hanley, C., Layne, J., Punnoose, A., Reddy, K.M., Coombs, I., Coombs, A., Feris, K., Wingett, D., 2008. Preferential killing of cancer cells and activated human T cells using ZnO nanoparticles. Nanotechnology. 19(29), 295103. DOI: 10.1088/0957-4484/19/29/295103.

Hanley, C., Thurber, A., Hanna, C., Punnoose, A., Zhang, J., Wingett, D.G., 2009. The Influences of Cell Type and ZnO Nanoparticle Size on Immune Cell Cytotoxicity and Cytokine Induction. Nanoscale Res Lett. 4(12), 1409-1420. DOI: 10.1007/s11671-009-9413-8.

Hartwig, A., 2001. Zinc finger proteins as potential targets for toxic metal ions: differential effects on structure and function. Antioxid Redox Signal. 3(4), 625-634. DOI: 10.1089/15230860152542970.

Huang da, W., Sherman, B.T., Lempicki, R.A., 2009. Systematic and integrative analysis of large gene lists using DAVID bioinformatics resources. Nat Protoc. 4(1):44-57. DOI: 10.1038/nprot.2008.211.

Hussien, R., Rihn B.H., Eidi, H., Ronzani, C., Joubert, O., Ferrari, L., Vazquez O., Kaufer, D., Brooks, G.A., 2013. Unique growth pattern of human mammary epithelial cells induced by polymeric nanoparticles. Physiol Rep. 422(1-2):495-503. DOI: 10.1016/j.ijpharm.2011.11.020

Jones, C.F., Grainger, D.W, 2009. In vitro assessments of nanomaterial toxicity. Adv Drug Deliv Rev. 61(6):438-456. DOI: 10.1016/j.addr.2009.03.005. Epub 2009

Joo, S.H., Zhao, D., 2017. Environmental dynamics of metal oxide nanoparticles in heterogeneous systems: A review. J Hazard Mater. 15(322)(Pt A), 29-47. DOI: 10.1016/j.jhazmat.2016.02.068.

Liang, H., He, T., Long, J., Liu, L., Liao, G., Ding, Y., Cao, Y., 2018. Influence of bovine serum albumin pre-incubation on toxicity and ER stress-apoptosis gene expression in THP-1 macrophages exposed to ZnO nanoparticles. Toxicol Mech Methods. 21, 1-12. doi: 10.1080/15376516.2018.1479907.

Mishra, P.K., Mishra, H., Ekielski, A., Talegaonkar, S., Vaidya, B., 2017. Zinc oxide nanoparticles: a promising nanomaterial for biomedical applications. Drug Discov Today. 22(12), 1825-1834. DOI: 10.1016/j.drudis.2017.08.006.

Moos, P.J., Olszewski, K., Honeggar, M., Cassidy, P., Leachman, S., Woessner, D., Cutler, N.S., Veranth, J.M., 2011. Responses of human cells to ZnO nanoparticles: a gene transcription study. Metallomics. 3(11), 1199-1211. DOI: 10.1039/c1mt00061f.

Phuyal, S., Kasem, M., Rubio, L., Karlsson, H.L., Marcos, R., Skaug, V., Zienolddiny, S., 2017. Effects on human bronchial epithelial cells following low-dose chronic exposure to nanomaterials: A 6-month transformation study. Toxicol In Vitro. 44:230-240. doi: 10.1016/j.tiv.2017.07.016.

Prach, M., Stone, V., Proudfoot, L., 2013. Zinc oxide nanoparticles and monocytes: impact of size, charge and solubility on activation status. Toxicol Appl Pharmacol. 266(1),19-26. DOI: 10.1016/j.taap.2012.10.020.

Premanathan, M., Karthikeyan, K., Jeyasubramanian, K., Manivannan, G., 2011. Selective toxicity of ZnO nanoparticles toward Gram-positive bacteria and cancer cells by apoptosis through lipid peroxidation. Nanomedicine. 7(2),184-192. DOI: 10.1016/j.nano.2010.10.001.

Reed, L.J, Muench, H., 1938. A simple method of estimating fifty percent endpoints. The American Journal of Hygien. 27, 493–497.

Rihn, B.H., Joubert, O., 2015. Comment on "Protein Corona Fingerprinting Predicts the Cellular Interaction of Gold and Silver Nanoparticles". ACS Nano. 9(6), 5634-5635. DOI: 10.1021/acsnano.5b00459.

Ronzani, C., Safar, R., Diab, R., Chevrier, J., Paoli, J., Abdel-Wahhab, M.A., Le Faou, A., Rihn, B.H., Joubert, O., 2014. Viability and gene expression responses to polymeric nanoparticles in human and rat cells. Cell Biol Toxicol. 30(3), 137-146. DOI: 10.1007/s10565-014-9275-4.

Roy, R., Parashar, V., Chauhan, L.K., Shanker, R., Das, M., Tripathi, A., Dwivedi, P.D., 2014. Mechanism of uptake of ZnO nanoparticles and inflammatory responses in macrophages require PI3K mediated MAPKs signaling. Toxicol In Vitro. 28(3), 457-467. DOI: 10.1016/j.tiv.2013.12.004.

Safar, R., Ronzani, C., Diab, R., Chevrier, J., Bensoussan, D., Grandemange, S., Le Faou, A., Rihn, B.H., Joubert, O., 2015. Human monocyte response to S-nitrosoglutathione-loaded

nanoparticles: uptake, viability, and transcriptome. Mol Pharm. 12(2):554-561. DOI: 10.1021/mp5006382.

Sahu, D., Kannan, G.M., Vijayaraghavan, R., 2014. Size-dependent effect of zinc oxide on toxicity and inflammatory potential of human monocytes. J Toxicol Environ Health A. 77(4), 177-191. DOI: 10.1080/15287394.2013.853224.

Senapati, V.A., Kumar, A., Gupta, G.S., Pandey, A.K., Dhawan, A., 2015. ZnO nanoparticles induced inflammatory response and genotoxicity in human blood cells: A mechanistic approach. Food Chem Toxicol. 85, 61-70. DOI: 10.1016/j.fct.2015.06.018.

Sze, A, Erickson D, Ren L, Li D. Zeta-potential measurement using the Smoluchowski equation and the slope of the current-time relationship in electroosmotic flow. J Colloid Interface Sci. 2003 May 15;261(2):402-10. PubMed PMID: 16256549.

Szklarczyk, D., Franceschini, A., Wyder, S., Forslund, K., Heller, D., Huerta-Cepas, J., Simonovic, M., Roth, A., Santos, A., Tsafou, K.P., Kuhn, M., Bork, P., Jensen, L.J., von Mering, C., 2015. STRING v10: protein-protein interaction networks, integrated over the tree of life. Nucleic Acids Res. 43(Database issue), D447-452. DOI: 10.1093/nar/gku1003.

Tuomela, S., Autio, R., Buerki-Thurnherr, T., Arslan, O., Kunzmann, A., Andersson-Willman, B., Wick, P., Mathur, S., Scheynius, A., Krug, H.F., Fadeel, B., Lahesmaa, R., 2013. Gene

expression profiling of immune-competent human cells exposed to engineered zinc oxide or titanium dioxide nanoparticles. PLoS One. 8(7), e68415. DOI: 10.1371/journal.pone.0068415.

Vance, M.E., Kuiken, T., Vejerano, E.P., McGinnis, S.P., Hochella, M.F. Jr., Rejeski, D., Hull, M.S., 2015. Nanotechnology in the real world: Redeveloping the nanomaterial consumer products inventory. Beilstein J Nanotechnol. 21(6), 1769-1780. DOI: 10.3762/bjnano.6.181. eCollection 2015.

Wang, B., Zhang, J., Chen, C., Xu, G., Qin, X., Hong, Y., Bose, D.D., Qiu, F., Zou, Z., 2018. The size of zinc oxide nanoparticles controls its toxicity through impairing autophagic flux in A549 lung epithelial cells. Toxicol Lett. 285, 51-59. DOI: 10.1016/j.toxlet.2017.12.025

Wilhelmi, V., Fischer, U., Weighardt, H., Schulze-Osthoff, K., Nickel, C., Stahlmecke, B., Kuhlbusch, T.A., Scherbart, A.M., Esser, C., Schins, R.P., Albrecht, C., 2013. Zinc oxide nanoparticles induce necrosis and apoptosis in macrophages in a p47phox- and Nrf2-independent manner. PLoS One. 8(6), e65704. DOI: 10.1371/journal.pone.0065704

Yin, H., Casey, P.S., McCall, M.J., Fenech, M., 2015. Size-dependent cytotoxicity and genotoxicity of ZnO particles to human lymphoblastoid (WIL2-NS) cells. Environ Mol Mutagen. 56(9), 767-776. DOI: 10.1002/em.21962.

Tables

Table 1: Numbers of PMA-differentiated THP-1 genes having at least 1.5 fold change up or down regulated ($p \leq 0.05$) after exposure to both high and low concentrations of ZnO110NP, namely, 8.1 µg/mL = 2.1 µg/cm^2 (IC_{50}) and 2.0 µg/mL = 0.5 µg/cm^2 ($IC_{50}/4$). Data from three independent experiments was normalized using GeneSpring and submitted to a *t*.test student following Benjamini-Hochberg correction.

	$IC_{50}/4$	**IC_{50}**
All genes	360	3202
Up-regulated genes	33	872
Down-regulated genes	327	2330

Table 2: Common significant ($p \leq 0.05$) up-regulated genes with their Fold Change following exposure of PMA-differentiated THP-1 cells to both high and low concentrations of ZnO110NP.

		Fold Change	
Gene Symbol	**Gene Name**	**$IC_{50}/4$**	**IC_{50}**
HSPA6	Heat shock 70kDa protein 6	81.53	6912.33
MT1M	Metallothionein 1M	56.88	57.64
MT1E	Metallothionein 1E	34.34	44.76
MT1H	Metallothionein 1H	28.91	83.36
MT1X	Metallothionein 1X	28.40	44.55
MT1G	Metallothionein 1G	26.15	57.57
MT1L	Metallothionein 1L	23.55	29.40
MT1B	Metallothionein 1B	22.87	73.67
MT1HL1	Metallothionein 1H-like 1	17.37	69.38
HSPA1A	Heat shock 70kDa protein 1A	16.73	1586.45
MT1A	Metallothionein 1A	12.21	33.17
MT2A	Metallothionein 2A	12.16	7.24
FAM189A2	Family with sequence similarity 189, member A2	9.68	4.45
HSPA1B	Heat shock 70kDa protein 1B	9.42	461.72
WNT6	Wingless-type MMTV integration site family, member 6	7.27	20.87
ASCL2	Achaete-scute family bHLH transcription factor 2	6.08	4.93
ZBTB2	Zinc finger and BTB domain containing 2	5.60	2.97
ASB13	Ankyrin repeat and SOCS box containing 13	5.58	4.37
MT1F	Metallothionein 1F	4.63	3.45
SLC30A1	Solute carrier family 30 (zinc transporter), member 1	4.44	5.71
HMOX1	Heme oxygenase (decycling) 1	2.86	2.76
CDCA7L	Cell division cycle associated 7-like	2.61	3.04
CNKSR3	CNKSR family member 3	2.17	1.92
WFS1	Wolfram syndrome 1 (wolframin)	2.06	2.71
DMRTA2	DMRT-like family A2	1.91	1.58
GPANK1	G patch domain and ankyrin repeats 1	1.74	2.17
CCNE1	Cyclin E1	1.56	2.26

Figures

Figure 1: Zinc oxide nanoparticles NM110 (ZnO110NP) characterization. (A): size and (B): zeta potential as measured by DLS.

Figure 2: Cell phenotype study of THP-1 cells differentiated into macrophages by incubation for 24 h with (10 ng/mL = 16 nM) of phorbol 12-myistate 13-acetate (PMA). Cell differentiation was confirmed by flow cytometry using CD11c antibody. (A): Control, non-differentiated unstained cells (B): Cells not treated with PMA. (C): PMA treated cells.

Figure 3: Cytotoxic study of PMA treated THP-1 cells exposed to ZnO110NP as assessed by (A) WST-1 assay, (B) LDH assay, (C) AlamarBlue® assay. Un-exposed cells are considered as negative control, 100 % of cell viability. Data are expressed as mean ± S.E of four biological replicates. *** $p < 0.001$ et * $p < 0.05$

Figure 4: Functional annotations of significantly up- and down-regulated genes of PMA-differentiated THP-1 cells exposed to both high and low concentrations of ZnO110NP, namely, 8.1 µg/mL = 2.1 µg/cm^2 (IC_{50}) and 2.0 µg/mL = 0.5 µg/cm^2 (IC_{50}/4). On the left, the functional annotations (Biological process (GOTERM_BP) and pathways (KEGG, BIOCARTA)) obtained for IC_{50}/4 concentration, on the right the annotations obtained for IC_{50} concentration.

Figure 5: Significant upregulated genes of PMA-differentiated THP-1 cells exposed to both high and low concentrations of ZnO110NP, namely, 8.1 µg/mL = 2.1 µg/cm^2 (IC_{50}) and 2.0 µg/mL =

1 0.5 µg/cm^2 (IC_{50}/4) for 4h. (A) Venn diagram of the number of common and unique up-regulated
2 genes (at least 1.5-fold change and $p \leq 0.05$). (B) Interactions between the 27 common
3 upregulated genes as retrieved from the STRING database. Among them, we identified genes
4 belong to families: metallothioneins (*MT1, MT2*) and heat shock protein (*HSP*).

Supplementary informations

Figure S 1: Graphical representation of the principal component analysis (PCA) giving the distribution of analyzed samples by GeneSpring. Each condition (control, $IC_{50}/4$, IC_{50}) is represented by three independent experiments.

Figure S 2: Characterization of ZnO nanoparticles studied by transmission electron microscopy.

Table S 1: Full list of significant ($p \leq 0.05$) up-regulated genes following exposure of PMA-differentiated THP-1 cells to 2.0 µg/mL ($IC_{50}/4$) of ZnO110NP.

Table S 2: Full list of significant ($p \leq 0.05$) down-regulated genes following exposure of PMA-differentiated THP-1 cells to 2.0 µg/mL ($IC_{50}/4$) of ZnO110NP.

Table S 3: Full list of significant ($p \leq 0.05$) up-regulated genes following exposure of PMA-differentiated THP-1 cells to 8.1 µg/mL (IC_{50}) of ZnO110NP.

Table S 4: Full list of significant ($p \leq 0.05$) down-regulated genes following exposure of PMA-differentiated THP-1 cells to 8.1 µg/mL (IC_{50}) of ZnO110NP.

Table S 5: Significant clusters (Enrichment Score > 1.3) with Gene Ontology Biological Processes (GOTERM_BP) and pathways following exposure of PMA-differentiated THP-1 cells to 2.0 µg/mL ($IC_{50}/4$) of ZnO110NP.

Table S 6: Significant clusters (Enrichment Score > 1.3) with Gene Ontology Biological Processes (GOTERM_BP) and pathways following exposure of PMA-differentiated THP-1 cells to 8.1 µg/mL (IC_{50}) of ZnO110NP.

Table S 7: Characterization of ZnO nanoparticles by dynamic light scattering, after 0h or 24h in the medium of exposure (serum-free medium).

Table S 8: Measure of zinc (Zn) in the cell layers in contact with or inside the cells by Inductively Coupled Plasma-Optical Emission Spectrometer.

1 **Figure 1**

2

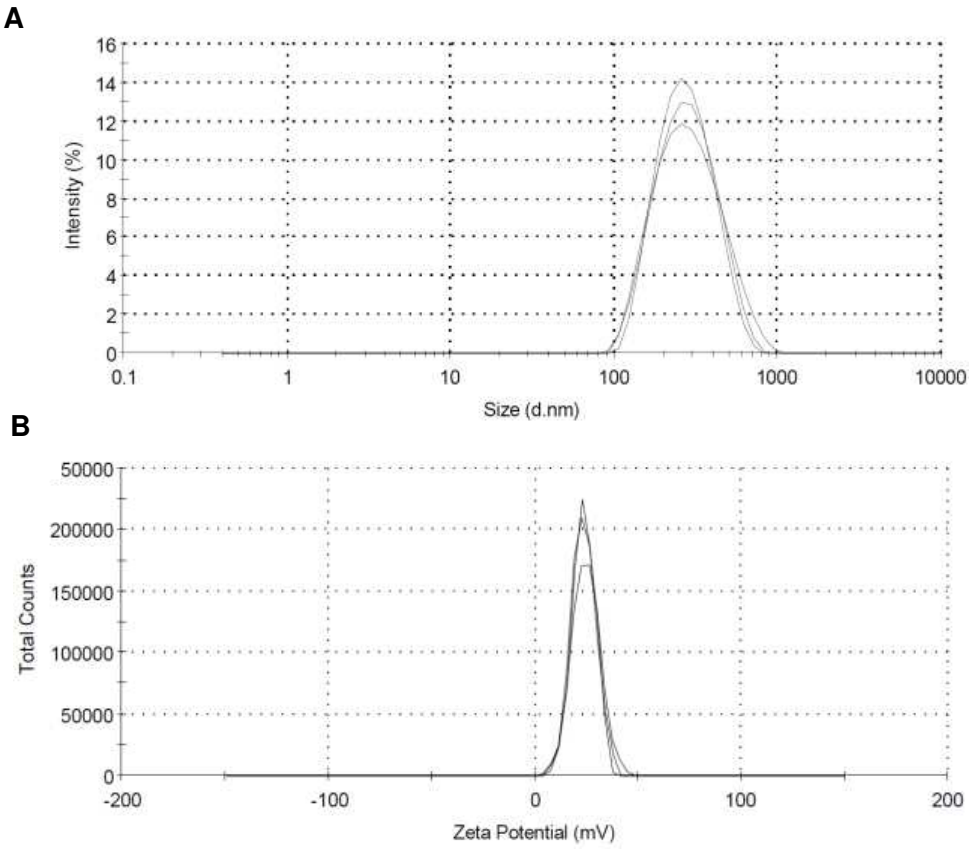
A
Intensity (%)
16
14
12
10
8
6
4
2
0
0.1
1
10
100
1000
10000
Size (d.nm)
B
Total Counts
50000
200000
150000
100000
50000
0
-200
-100
0
100
200
Zeta Potential (mV)

Figure 2

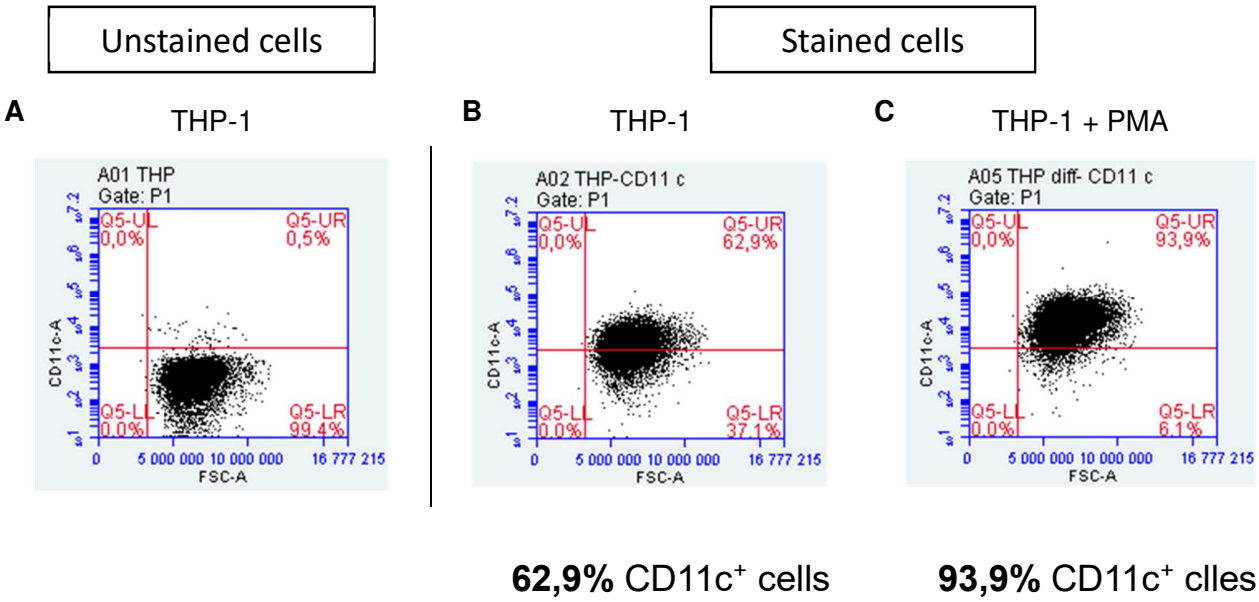
Unstained cells
Stained cells
A
THP-1
A01 THP
Gate: P1
Q5-UL
0,0%
Q5-UR
0,5%
Q5-LL
0,0%
Q5-LR
99,4%
B
THP-1
A02 THP-CD11 c
Gate: P1
Q5-UL
0,0%
Q5-UR
62,9%
Q5-LL
0,0%
Q5-LR
37,1%
C
THP-1 + PMA
A05 THP diff- CD11 c
Gate: P1
Q5-UL
0,0%
Q5-UR
93,9%
Q5-LL
0,0%
Q5-LR
6,1%
CD11c-A
FSC-A
0
5 000 000
10 000 000
16 777 215
62,9% CD11c+ cells
93,9% CD11c+ clles

Figure 3

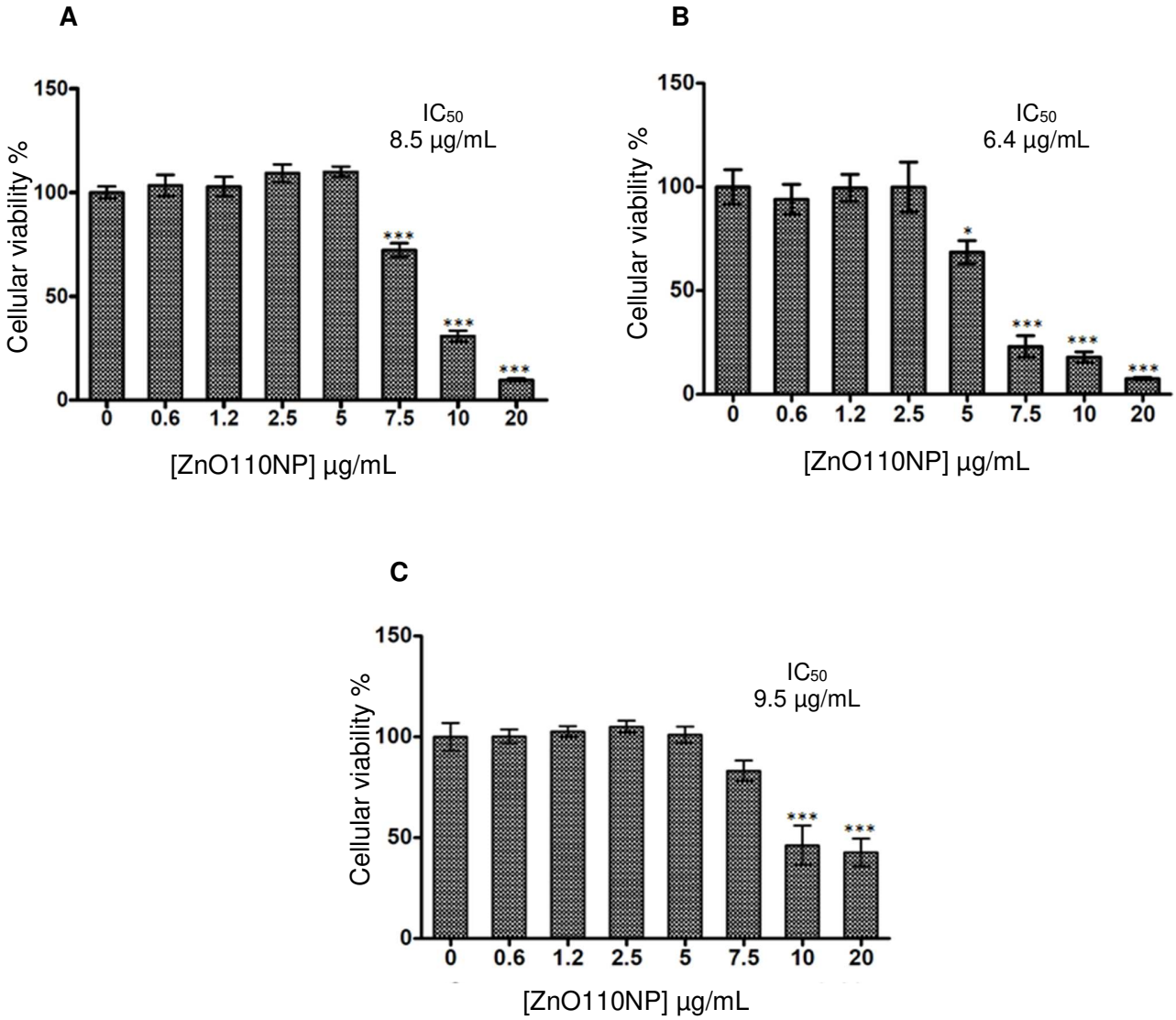
A
150
100
50
0
Cellular viability %
IC50
8.5 µg/mL
***
***
***
0
0.6
1.2
2.5
5
7.5
10
20
[ZnO110NP] µg/mL
B
150
100
50
0
Cellular viability %
IC50
6.4 µg/mL
*
***
***
***
0
0.6
1.2
2.5
5
7.5
10
20
[ZnO110NP] µg/mL
C
150
100
50
0
Cellular viability %
IC50
9.5 µg/mL
***
***
0
0.6
1.2
2.5
5
7.5
10
20
[ZnO110NP] µg/mL

Figure 4

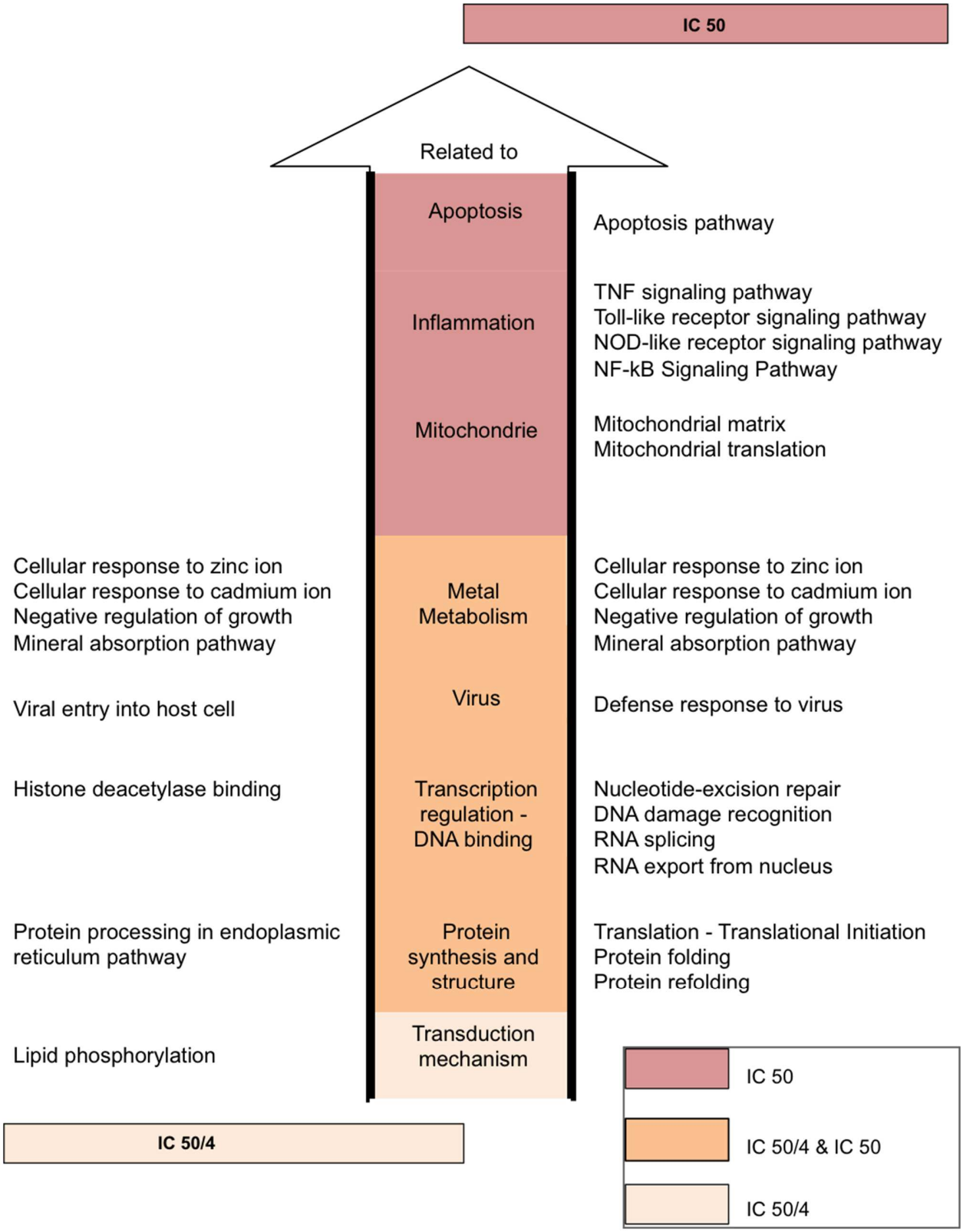
IC 50
Related to
Apoptosis
Apoptosis pathway
Inflammation
TNF signaling pathway
Toll-like receptor signaling pathway
NOD-like receptor signaling pathway
NF-kB Signaling Pathway
Mitochondrie
Mitochondrial matrix
Mitochondrial translation
Cellular response to zinc ion
Cellular response to cadmium ion
Negative regulation of growth
Mineral absorption pathway
Metal Metabolism
Cellular response to zinc ion
Cellular response to cadmium ion
Negative regulation of growth
Mineral absorption pathway
Viral entry into host cell
Virus
Defense response to virus
Histone deacetylase binding
Transcription regulation - DNA binding
Nucleotide-excision repair
DNA damage recognition
RNA splicing
RNA export from nucleus
Protein processing in endoplasmic reticulum pathway
Protein synthesis and structure
Translation - Translational Initiation
Protein folding
Protein refolding
Lipid phosphorylation
Transduction mechanism
IC 50/4
IC 50
IC 50/4 & IC 50
IC 50/4

Figure 5

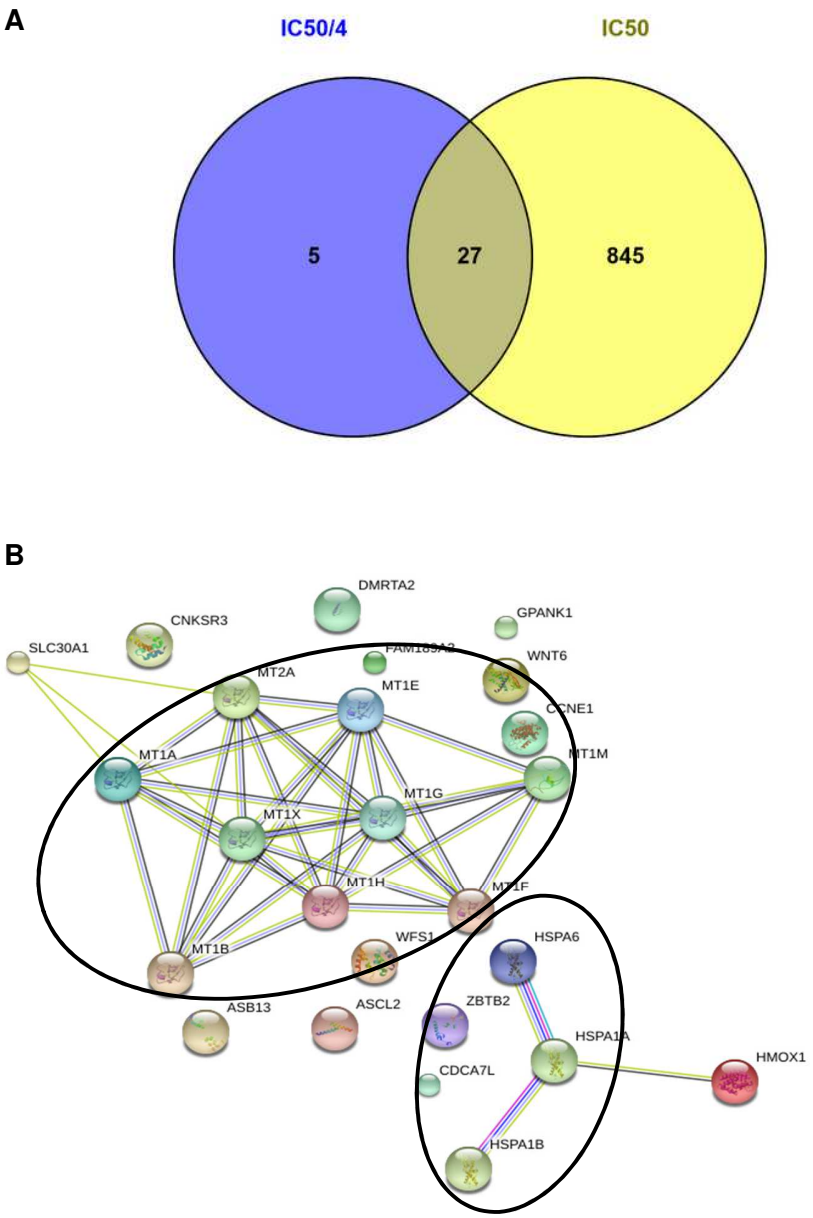
A
IC50/4
IC50
5
27
845
B
DMRTA2
GPANK1
CNKSR3
SLC30A1
WNT6
MT2A
MT1E
CCNE1
MT1A
MT1M
MT1G
MT1X
MT1H
MT1F
WFS1
HSPA6
MT1B
ASB13
ASCL2
ZBTB2
HSPA1A
HMOX1
CDCA7L
HSPA1B